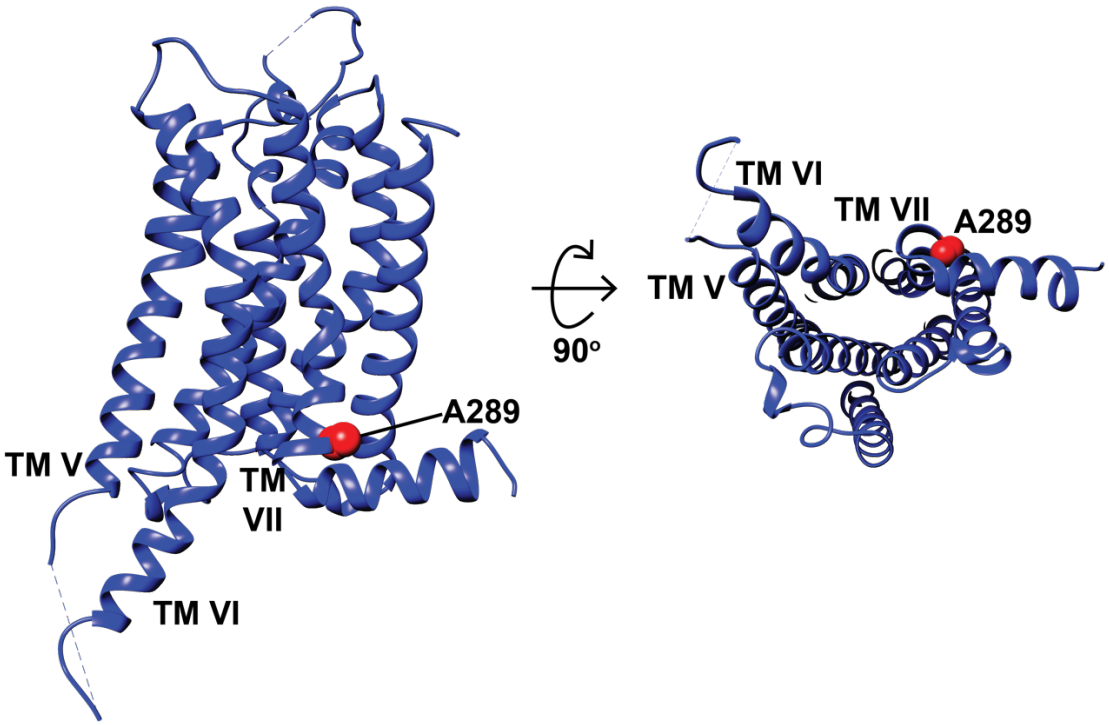

Figure S1. Location of ^{19}F-NMR probe in A_{2A}AR. Related to Figures 1 and 2.

Crystal structure of A_{2A}AR (PDB ID: 3EML) showing the location A289 (red sphere), which was replaced with cysteine for attachment of the ^{19}F-NMR probe.

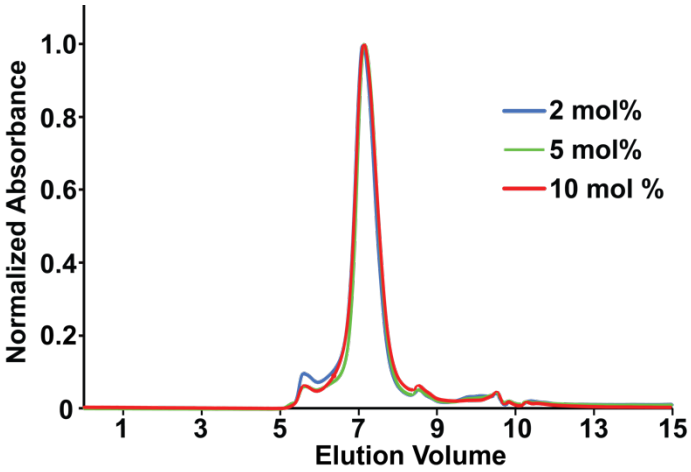

Figure S2. Characterization of A_{2A}AR in cholesterol containing nanodiscs. Related to Figure 1.

Superposition of analytical size exclusion chromatograms of A_{2A}AR in complex with NECA in nanodiscs containing POPC and POPS (70:30 molar ratio) and cholesterol at ratios of 2 mol% (blue), 5 mol% (green) and 10 mol% (red).

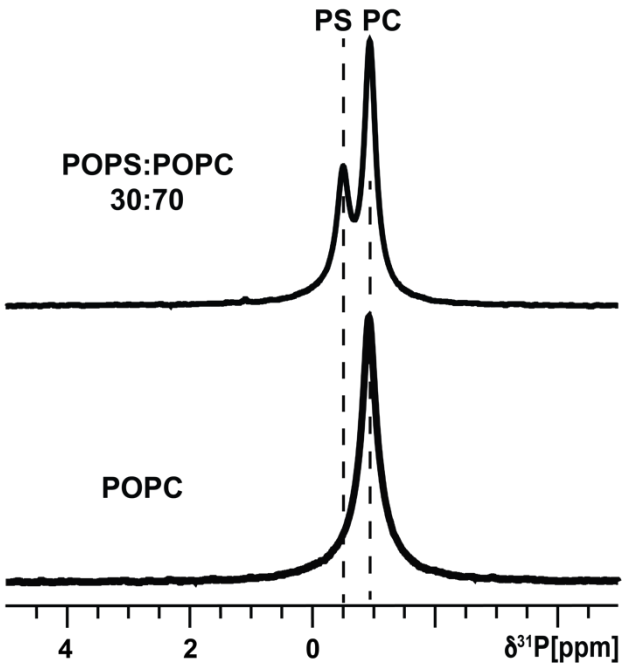

Figure S3. ^{31}P-NMR of lipid nanodiscs. Related to Figure 1.

1D ^{31}P NMR spectra of A_{2A}AR[A289C^{TET}] in nanodiscs containing POPC or POPC:POPS (70:30 molar ratio). The vertical dashed lines indicate the observed chemical shifts for the two lipid headgroups of POPC or POPS, which were consistent with manufacturer's reported values. The relative intensities of the two observed signals were quantitatively consistent with the expected lipid ratios in the nanodisc samples.

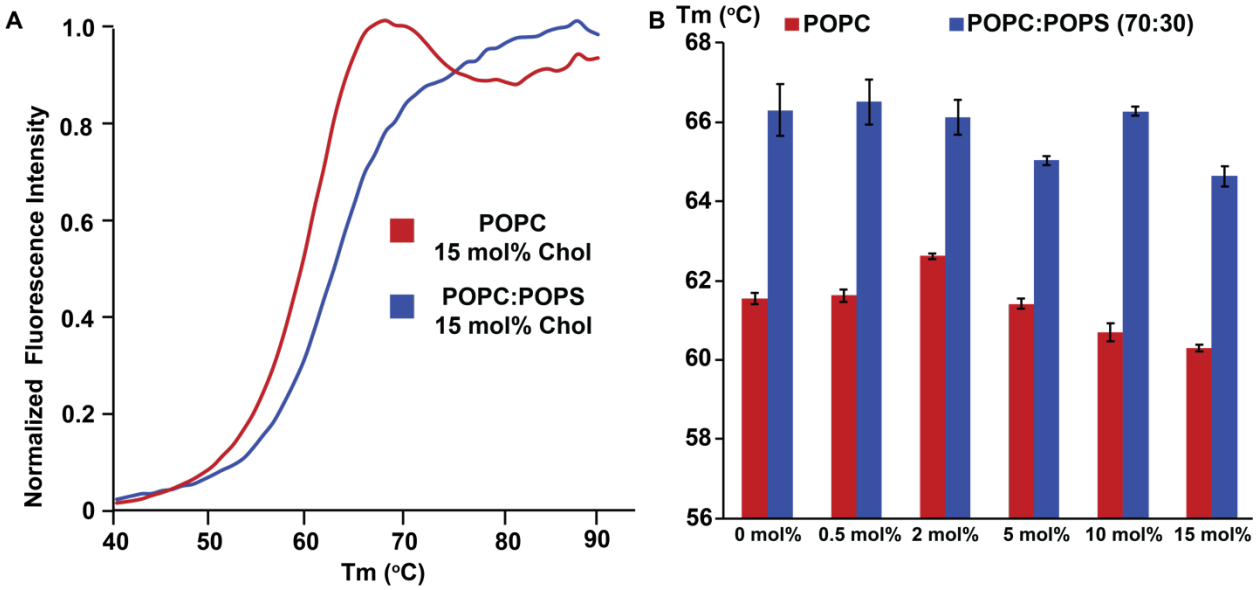

Figure S4. The global fold of A_{2A}AR[A289C] across the range of employed membrane compositions, as assessed by a fluorescence thermal shift assay. Related to Figure 1.

(A) Representative fluorescence curves for A_{2A}AR[A289C] in complex with NECA and in nanodiscs containing 15 mol% cholesterol and POPC (red curve) or POPC and POPS (70:30 molar ratio, blue curve). The melting temperatures (T_M) values were determined by fitting each curve to a Boltzman sigmoidal function (see STAR Methods). (B) Melting temperatures determined from fluorescence thermal shift assay of A_{2A}AR[A289C] in complex with NECA in nanodiscs containing either POPC (red bars) or POPC:POPS (70:30 molar ratio, blue bars) and varying amounts of cholesterol as indicated. Error bars for each sample were calculated as the standard error of mean (s.e.m) for 3 or more independent experiments.

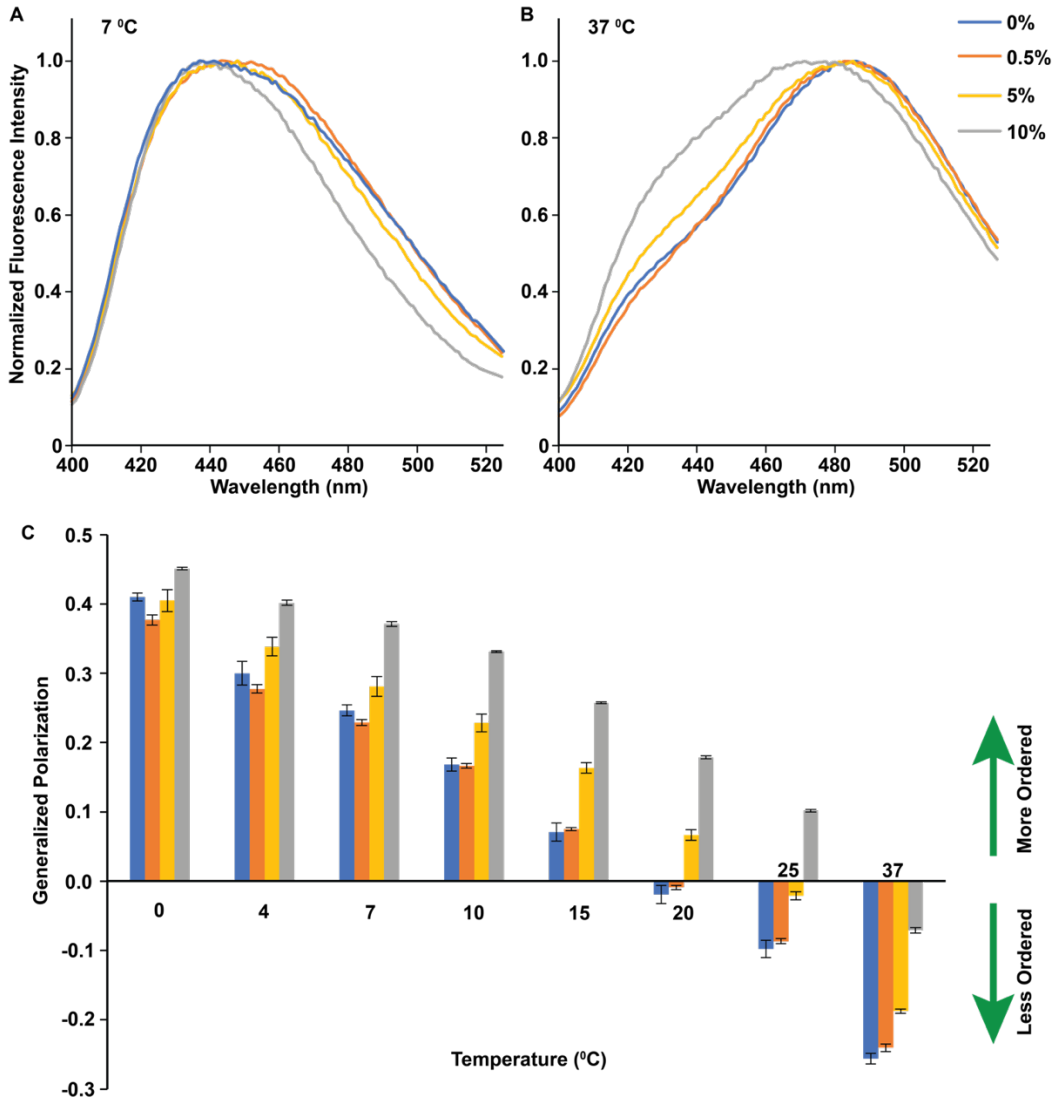

Figure S5. Fluidity measurements of membrane lipids in nanodiscs containing POPC and varying amounts of cholesterol. Related to Figure 2. (A and B) Superimposed normalized fluorescence intensity curves measured at (A) 7 °C, and (B) 37 °C for nanodisc samples containing POPC, Laurdan, and 0 mol% (blue), 0.5 mol% (orange), 5 mol% (yellow) or 10 mol% cholesterol (grey). (C) Generalized polarization values calculated from the plots in (A) and (B) and additional similar experiments

measured from 0 ºC to 37 ºC. Error bars indicate s.e.m. calculated from n=3 independent experiments.

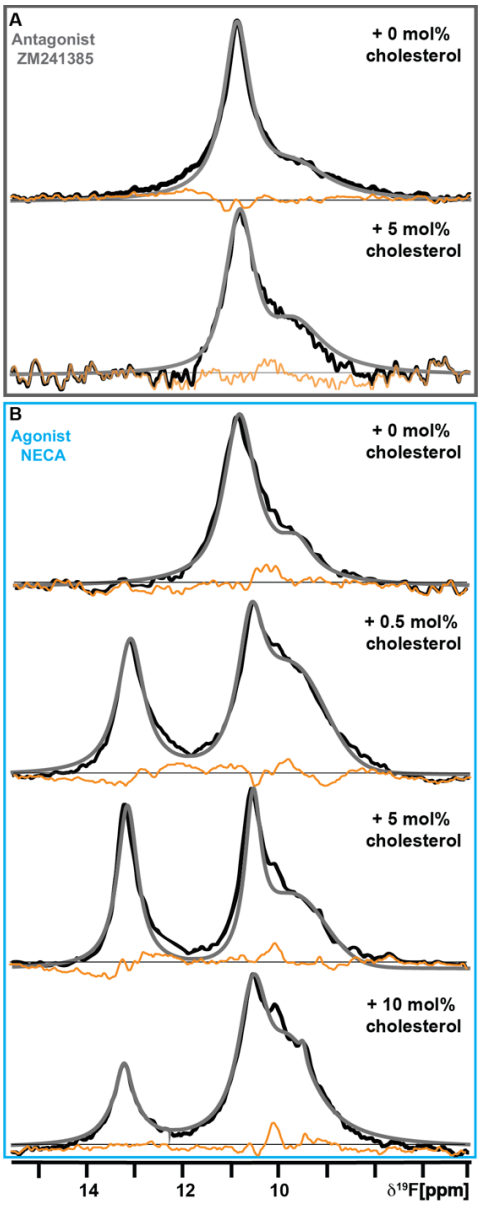

Figure S6. Residual differences between the raw data and summation of the individually fit components from Figure 2. Related to Figure 2. The experimental data are shown in black, the grey lines superimposed on the spectra are the total sums of the individual deconvolutions, and the orange line is the calculated difference between the grey and black lines. Minor features visible in the residual were recognized as either noise or minor impurities that did not impact the fit of the clearly visible signals from the receptor and thus were not assigned.

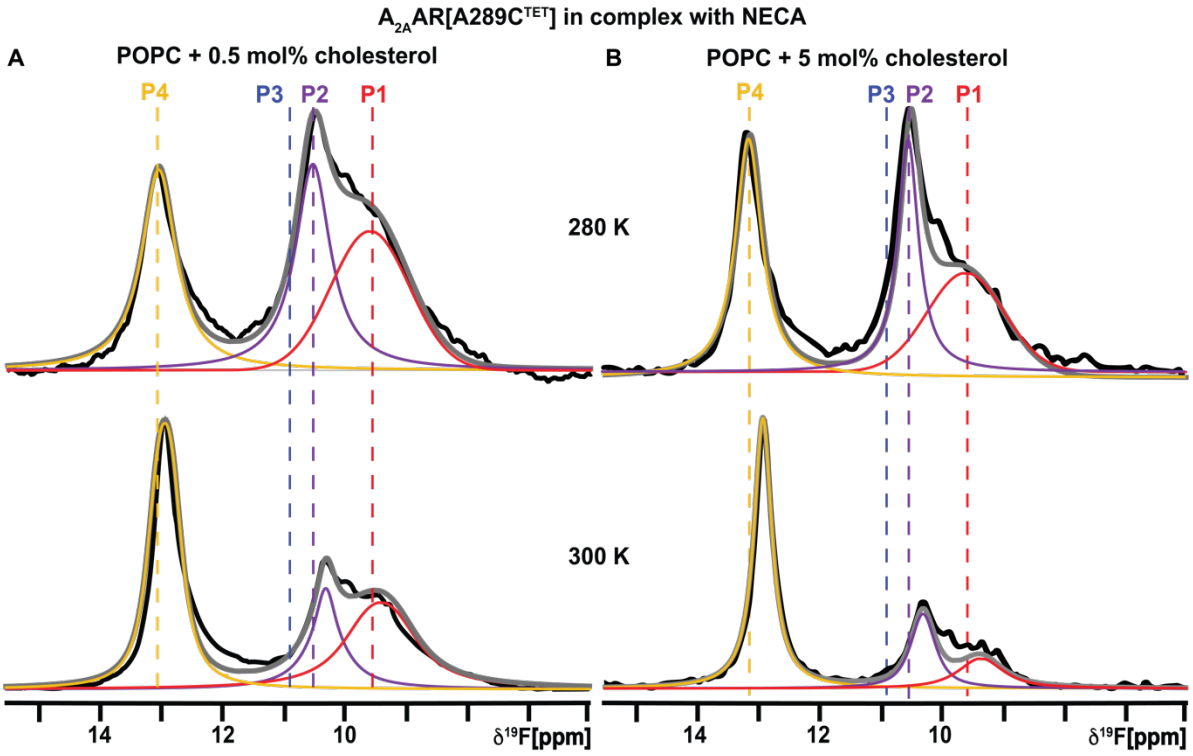

Figure S7. **The impact of temperature on the conformational equilibria of agonist-bound A_{2A}AR in nanodiscs containing POPC and varying amounts of cholesterol. Related to Figure 2.**

1-dimensional ^{19}F-NMR spectra of A_{2A}AR[A289C^{TET}] in complex with agonist NECA in nanodiscs containing POPC and (A) 0.5 mol% cholesterol or (B) 5 mol% cholesterol, recorded at 280 K (top) and 300 K (bottom). Other presentation details are the same as in Figure 2.

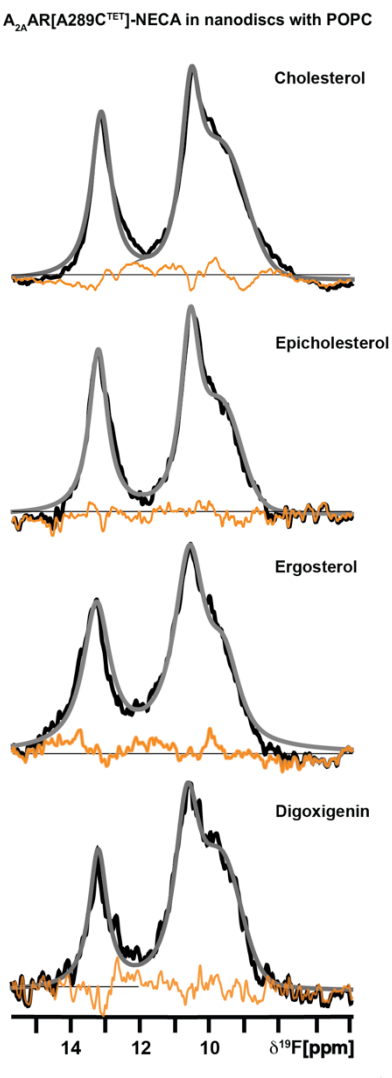

Figure S8. Residual differences between the raw data and summation of the individually fit components from Figure 3. Related to Figure 3. The experimental data are shown in black, the grey lines superimposed on the spectra are the total sums of the individual deconvolutions, and the orange line is the calculated difference between the grey and black lines.

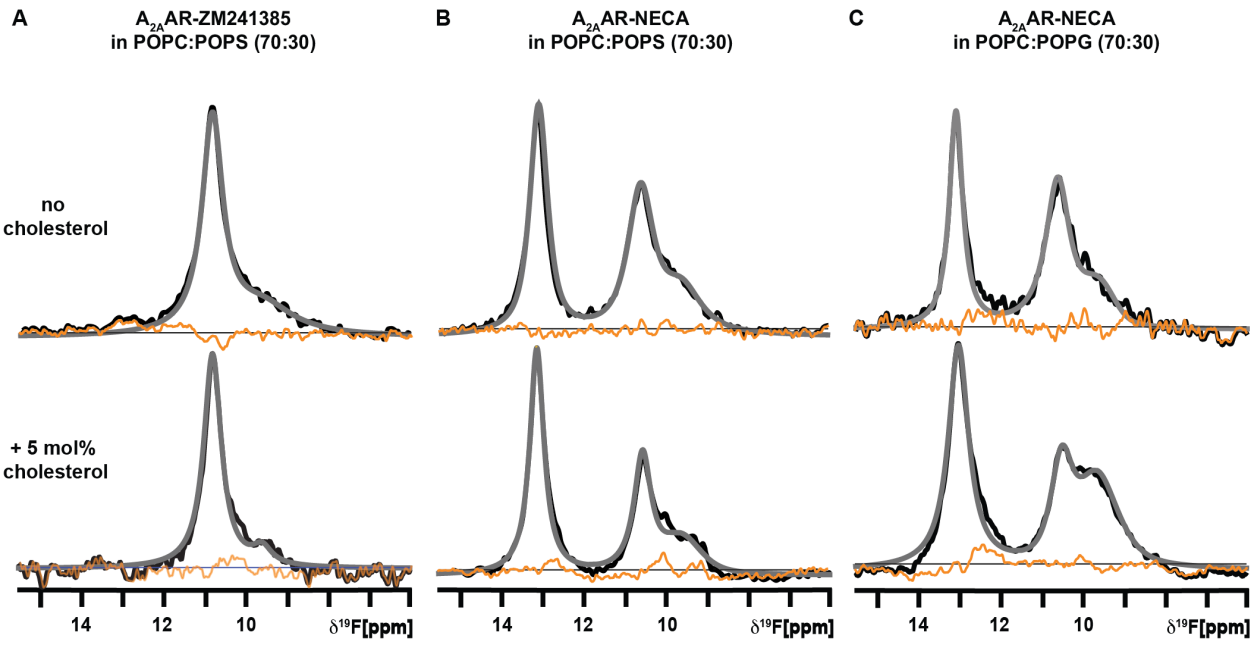

Figure S9. Residual differences between the raw data and summation of the individually fit components from Figure 4. Related to Figure 4. The experimental data are shown in black, the grey lines superimposed on the spectra are the total sums of the individual deconvolutions, and the orange line is the calculated difference between the grey and black lines.

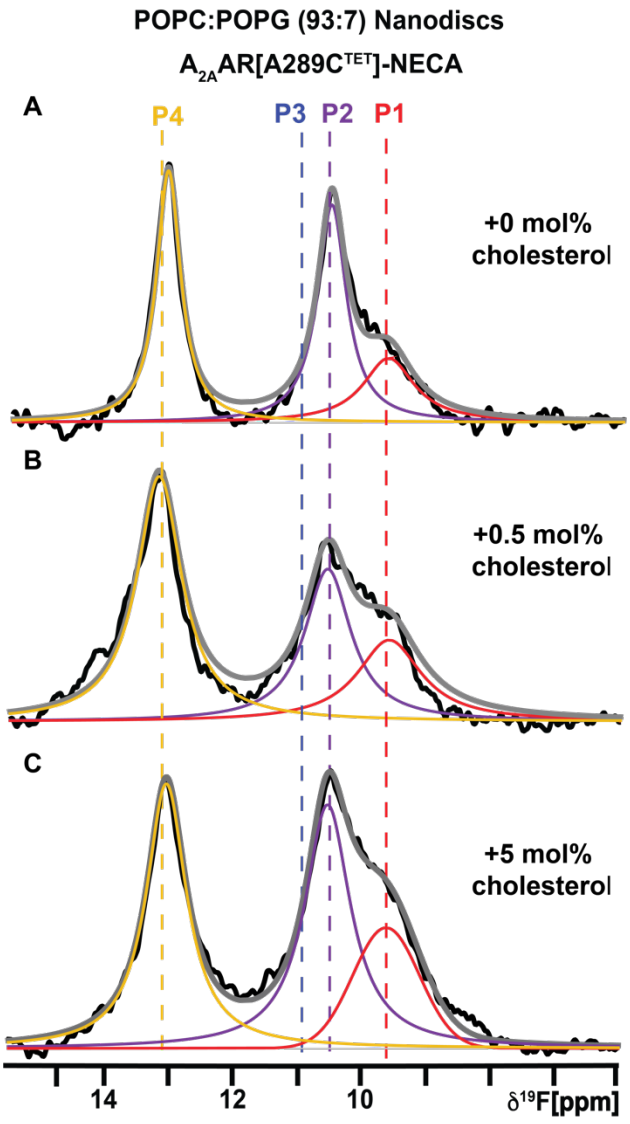

Figure S10. **The impact of cholesterol on the conformational equilibria of agonist-bound A_{2A}AR in nanodiscs containing POPC and POPG. Related to Figure 4.**

1-dimensional ^{19}F-NMR spectra of A_{2A}AR[A289C^{TET}] in complex with agonist NECA in nanodiscs containing POPC:POPG (93:7 molar ratio) and in the presence of (A) no cholesterol, (B) 0.5 mol% cholesterol and (C) 5 mol% cholesterol. Other presentation details are the same as in Figure 2.

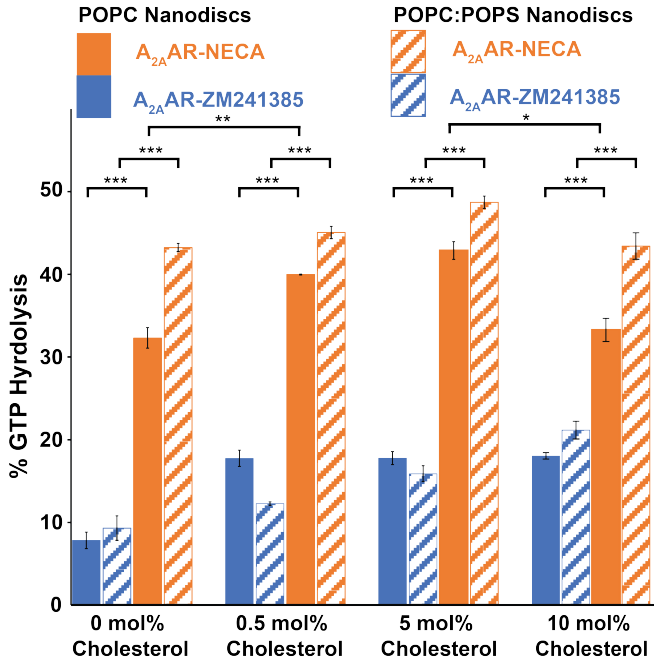

Figure S11. The impact of cholesterol and anionic phospholipids on GTP hydrolysis rates. Related to Figure 2 and Figure 4.

Results from the GTPase-Glo assay, reporting on GTP hydrolysis with $G\alpha_S$ in the presence of A_{2A}AR[A289C]-ligand complexes in nanodiscs of different lipid compositions. The percent GTP hydrolysis is shown for $G\alpha_S$ in the presence of A_{2A}AR in complex with the agonist NECA (solid and striped orange bars) and A_{2A}AR in complex with the antagonist ZM241385 (solid and striped blue bars). Measurements were done for A_{2A}AR in nanodiscs containing POPC (solid bars) or POPC:POPS (70:30 molar ratio, striped bars) with varying amounts of cholesterol, as indicated. Error bars indicate s.e.m. calculated from $n \geq 3$ independent experiments. Statistically significant values are illustrated as *P<0.05, **P<0.005, and ***P<0.0005 respectively using a 2-tailed unpaired t-test.

Table S1. Analytical determination of amount of cholesterol in nanodiscs. Related to STAR Methods and Figure 1.

Amounts of cholesterol in lipid nanodiscs determined using the Amplex® Red Cholesterol Assay[1] with nanodiscs containing POPC or mixtures of POPC and POPS over the range of fractions of cholesterol employed in this study. The values reported represent the mean ± s.e.m. calculated for $n \geq 3$ independent experiments.

Phospholipid composition	Target mol% of cholesterol	Observed mol% of cholesterol
POPC	0.5	0.67 ± 0.20
	2	1.92 ± 0.14
	5	4.89 ± 0.41
	10	10.07 ± 0.48
POPC:POPS (70:30)	0.5	0.70 ± 0.25
	2	2.03 ± 0.19
	5	5.03 ± 0.44
	10	10.5 ±0.44

Table S2. K_D and K_I values for the antagonist ZM241385 and agonist NECA. Related to Figure 1.

K_D and K_I values for the antagonist ZM241385 and agonist NECA, respectively, for A_{2A}AR[A289C] in nanodiscs containing POPC and varying amounts of cholesterol. The values were determined from the data plotted in Figure 1, and the reported error represents the s.e.m. for 3 independent trials done in triplicate.

Amount of cholesterol	K_D (for ZM241385) (nM)	K_I (for NECA) (nM)
0 mol%	1.01 ± 0.06	556 ± 122
2 mol%	2.76 ± 0.02	266 ± 24.8
5 mol%	3.18 ± 0.46	240 ± 67.3
10 mol%	1.31 ± 0.17	126 ± 8.32

Table S3. GTP hydrolysis of A_{2A}AR in lipid nanodiscs. Related to Figure 2, Figure 4 and Figure S7.

Percent GTP Hydrolysis of A_{2A}AR[A289C] in complex with antagonist (ZM241385) and agonist (NECA) in various lipid environments, as determined from the data plotted in Figure S7. Values reported are the means ± the s.e.m. determined from 3 or more independent replicates. Results from a statistical t-test analysis are reported in Figure S7.

Sample	Lipid composition	%GTP Hydrolysis
0 mol% Cholesterol		
A_{2A}AR-ZM241385	POPC	7.84 ± 1.00
	POPC:POPS	9.32 ± 1.47
A_{2A}AR-NECA	POPC	32.32 ± 1.23
	POPC:POPS	43.85 ± 0.49
0.5 mol% Cholesterol		
A_{2A}AR-ZM241385	POPC	17.75 ± 0.98
	POPC:POPS	12.28 ± 0.21
A_{2A}AR-NECA	POPC	39.98 ± 0.05
	POPC:POPS	45.07 ± 0.74
5 mol% Cholesterol		
A_{2A}AR-ZM241385	POPC	17.78 ± 0.77
	POPC:POPS	15.89 ± 0.95
A_{2A}AR-NECA	POPC	42.89 ± 1.07
	POPC:POPS	48.72 ± 0.75
10 mol% Cholesterol		
A_{2A}AR-ZM241385	POPC	18.12 ± 0.39
	POPC:POPS	21.25 ± 1.08
A_{2A}AR-NECA	POPC	33.46 ± 1.41
	POPC:POPS	43.67 ± 1.62

Table S4: Relative populations of the $A_{2A}AR$ conformational states observed in ^{19}F-NMR. Related to Figure 2, Figure 3, Figure 4, Figure 5 and Figure S6

The relative populations of the different $A_{2A}AR$ conformational states as observed in the ^{19}F-NMR spectra are reported here. The value reported for each conformation is a ratio of the integrated area of the specific deconvoluted peak to the total integral of all signals from 7.5 ppm to 14.5 ppm.

Sample	P4	P3	P2	P1
$A_{2A}AR$[A289C]-ZM241385 in POPC	0.00	0.68	0.00	0.32
$A_{2A}AR$[A289C]-ZM241385 in POPC + 5 mol% cholesterol	0.00	0.56	0.00	0.44
$A_{2A}AR$[A289C]-NECA in POPC	0.00	0.70	0.13	0.17
$A_{2A}AR$[A289C]-NECA in POPC + 0.5 mol% cholesterol	0.31	0.00	0.25	0.44
$A_{2A}AR$[A289C]-NECA in POPC + 5 mol% cholesterol	0.40	0.00	0.30	0.31
$A_{2A}AR$[A289C]-NECA in POPC + 10 mol% cholesterol	0.18	0.00	0.37	0.45
$A_{2A}AR$[A289C]-NECA in POPC + 0.5 mol% epi-cholesterol	0.37	0.00	0.39	0.24
$A_{2A}AR$[A289C]-NECA in POPC + 0.5 mol% ergosterol	0.33	0.00	0.52	0.15
$A_{2A}AR$[A289C]-NECA in POPC + 0.5 mol% digoxigenin	0.19	0.00	0.55	0.26
$A_{2A}AR$[A289C]-ZM241385 in POPC:POPS (70:30)	0.00	0.71	0.00	0.29
$A_{2A}AR$[A289C]-ZM241385 in POPC:POPS (70:30) + 5 mol% cholesterol	0.00	0.85	0.00	0.15
$A_{2A}AR$[A289C]-NECA in POPC:POPS (70:30)	0.43	0.00	0.39	0.17
$A_{2A}AR$[A289C]-NECA in POPC:POPS (70:30) + 5 mol% cholesterol	0.51	0.00	0.32	0.17
$A_{2A}AR$[A289C]-NECA in POPC:POPG (70:30)	0.41	0.00	0.37	0.22
$A_{2A}AR$[A289C]-NECA in POPC:POPG (70:30) + 5 mol% cholesterol	0.47	0.00	0.19	0.34
$A_{2A}AR$[R291Q,A289C]-NECA in POPC + 0.5 mol% cholesterol	0.14	0.00	0.37	0.49
$A_{2A}AR$[W129I,A289C]-NECA in POPC + 0.5 mol% cholesterol	0.26	0.00	0.02	0.71
$A_{2A}AR$[A289C]-NECA in POPC:POPG (93:7)	0.39	0.00	0.40	0.21

A_{2A}AR[A289C]-NECA in POPC:POPG (93:7) + 0.5 mol% cholesterol	0.47	0.00	0.30	0.23
A_{2A}AR[A289C]-NECA in POPC:POPG (93:7) + 5 mol% cholesterol	0.39	0.00	0.41	0.20
A_{2A}AR[A289C]-NECA in POPC + 0.5 mol% cholesterol at 300 K	0.45	0.00	0.20	0.35
A_{2A}AR[A289C]-NECA in POPC + 5 mol% cholesterol at 300 K	0.62	0.00	0.22	0.16

References

1. Amundson, D.M., and Zhou, M. (1999). Fluorometric method for the enzymatic determination of cholesterol. Journal of Biochemical and Biophysical Methods *38*, 43-52. 10.1016/S0165-022X(98)00036-0.